Biomaterials Science

ROYAL SOCIETY OF CHEMISTRY

PAPER

View Article Online
View Journal | View Issue

Check for updates

Cite this: *Biomater. Sci.*, 2022, **10**, 3845

Thermosensitive hydrogels to deliver reactive species generated by cold atmospheric plasma: a case study with methylcellulose†

Xavi Solé-Martí, [a,b,c] Tània Vilella,[a,b] Cédric Labay,[a,b,c] Francesco Tampieri, [a,b,c] Maria-Pau Ginebra [a,b,d] and Cristina Canal *[a,b,c]

Hydrogels have been recently proposed as suitable materials to generate reactive oxygen and nitrogen species (RONS) upon gas-plasma treatment, and postulated as promising alternatives to conventional cancer therapies. Acting as delivery vehicles that allow a controlled release of RONS to the diseased site, plasma-treated hydrogels can overcome some of the limitations presented by plasma-treated liquids in *in vivo* therapies. In this work, we optimized the composition of a methylcellulose (MC) hydrogel to confer it with the ability to form a gel at physiological temperatures while remaining in the liquid phase at room temperature to allow gas-plasma treatment with suitable formation of plasma-generated RONS. MC hydrogels demonstrated the capacity for generation, prolonged storage and release of RONS. This release induced cytotoxic effects on the osteosarcoma cancer cell line MG-63, reducing its cell viability in a dose-response manner. These promising results postulate plasma-treated thermosensitive hydrogels as good candidates to provide local anticancer therapies.

Received 28th February 2022,
Accepted 12th May 2022

DOI: 10.1039/d2bm00308b

rsc.li/biomaterials-science

1 Introduction

Plasma-treated liquids (PTLs) are produced when the reactive oxygen and nitrogen species (RONS) generated from a gas-plasma source are transferred to a liquid medium.[1,2] Research in this field has shown that PTLs can be used to target malignant tumors and selectively kill cancer cells without damaging surrounding healthy cells/tissues.[3–6] For this reason, anticancer therapies based on PTLs have moved forward during the last few years, reporting beneficial effects already in *in vivo* models.[7] Compared to direct treatment with gas plasmas, PTLs represent a promising alternative when treating malignant tumors located in internal organs, which would require open surgery to be treated with a gas-plasma device.[8] Therefore, in view of translation of this technology to the clinic, the development of PTLs that can be stored and administered by injection to the tumor would be a very valuable asset. However, the injection of a liquid to the tumor site might result in fast diffusion throughout the whole body due to blood flow, thus reducing the efficiency and efficacy of the PTL treatment. Besides, multiple PTL injections are needed to induce biological effects *in vivo*.[9–12] For these reasons, new strategies with hydrogel-forming polymer solutions are under investigation, with the aim of designing new efficient vehicles that allow a localized release of RONS directly to the tumor site.[13–15] In these studies, gelatin and alginate solutions were reported not only to foster the generation of RONS compared to certain saline solutions, but also to be suitable vehicles for the delivery of RONS, inducing cytotoxic effects to cancer cells without affecting nonmalignant cells. The latter show ionic crosslinking of the alginate chains in the presence of divalent cations like Ca^{2+}, but these and other strategies based on adding crosslinkers can have some drawbacks such as washout of the RONS generated by the plasma treatment.[13] Recently, a thermosensitive synthetic hydrogel based on polylactide and polyethyleneglycol and undergoing *in situ* gel formation has also been investigated as a RONS delivery vehicle.[16] By modulating their sol-gel transition temperature, thermosensitive hydrogels can be conveniently injected with minimal invasive surgery and also fill irregular shaped defects, sometimes created after a tumor resection. Methylcellulose (MC) is a water-soluble cellulose derivative that can form a thermoreversible hydrogel in water upon heating. At low temperature water molecules form a cage-like structure surrounding

[a]*Biomaterials, Biomechanics and Tissue Engineering Group, Department of Materials Science and Engineering, and Research Centre for Biomedical Engineering (CREB), Universitat Politècnica de Catalunya (UPC), c/Eduard Maristany 14, 08019 Barcelona, Spain. E-mail: cristina.canal@upc.edu; Tel: +34 934 017 810*
[b]*Barcelona Research Center in Multiscale Science and Engineering, UPC, 08019 Barcelona, Spain*
[c]*Institut de Recerca Sant Joan de Déu, Santa Rosa 39-57, 08950 Esplugues de Llobregat, Spain*
[d]*Institute for Bioengineering of Catalonia (IBEC), Barcelona Institute of Science and Technology (BIST), c/Baldiri i Reixach 10-12, 08028 Barcelona, Spain*
† Electronic supplementary information (ESI) available. See DOI: https://doi.org/10.1039/d2bm00308b

the methoxy groups and thus solubilizing MC.[17–19] However, high temperatures cause the destruction of the cage structure of water and a three-dimensional hydrogel network is formed due to hydrophobic interactions of the methoxy groups of MC. The sol-gel transition temperature of pure MC is ~60 °C, too high for *in vivo* purposes.[20] However, the gel point can be altered by the addition of salts, based on the Hofmeister series.[21]

In this work, it is our aim to describe for the first time the ability of thermosensitive MC hydrogels to generate, store and release plasma-generated RONS for cancer treatment purposes. To do so, we optimized the composition of a MC hydrogel to confer the ability to form a gel at physiological temperatures while remaining in the liquid phase at room temperature to allow the suitable formation and homogeneous distribution of plasma-generated RONS. The effect of plasma treatment on MC physical–chemical properties are analyzed, together with the *in vitro* cytotoxic effects induced by the release of plasma-generated RONS to cancer cells.

2 Materials and methods

2.1 Sample preparation

Methylcellulose (Metolose® SM 4000, Shin-Etsu Chemical Co., Japan) with a methoxy content of 29.7% was used for the preparation of the hydrogels. MC solutions were prepared by dispersing the weighted MC powder with hot deionized water (approximately 80 °C) using the SpeedMixer™ (DAC 150.1 FVZ-k, 3500 rpm) for 5 minutes to obtain a homogeneous dispersion. Then, the solution was stirred with a magnetic stirrer inside an ice bath until a clear solution was obtained and stored in the refrigerator. Solutions containing di-sodium hydrogen phosphate (HP) ($Na_2HPO_4{\cdot}2H_2O$, purity >99.5%, Fluka) were prepared by mixing the salt with the MC powder prior to dissolution. All solutions were gently stirred for 15 minutes prior to testing. Samples were named *x*MC*y*HP, where *x* and *y* are the weight percent of MC and HP in the solution, respectively.

2.2 Plasma treatment

Plasma treatment of the different MC solutions was performed using a commercial plasma jet kINPen® IND (Neoplas tools GmbH, Germany) operated with Ar gas (Ar 5.0, PRAXAIR, Spain). Gas flow was set to 1 L min^{-1}. The treatments were done on 1000 μL of sample, in a 24-well plate, at 10 mm distance between the nozzle of the jet and the surface of the solution. Different plasma treatments (60, 180 and 300 s) were evaluated. During plasma treatment, MC solutions were magnetically stirred to ensure the homogeneous distribution of the generated reactive species (Fig. S1†).

2.3 Quantification of RONS

The generation of reactive species was quantified as reported in the protocol.[22] In brief, the determination of species such as NO_2^-, NO_3^-, H_2O_2 and OH radicals in MC solutions and release media (culture medium or phosphate buffered saline (PBS)) was performed as follows.

2.3.1 Nitrite ions (NO_2^-). NO_2^- concentration after plasma treatment was determined using the Griess reagent (GR).[23–25] The GR was prepared by dissolving 0.1 wt% of *N*-(1-naphthyl) ethylenediamine dihydrochloride (Sigma Aldrich, USA), 1 wt% of sulfanilamide (Sigma Aldrich, USA) and 5 wt% of *ortho*-phosphoric acid 85% (Panreac, USA) in deionized water. 100 μL of GR were added to 100 μL of plasma-treated solutions of MC. Absorbance measurement at λ = 540 nm was performed with a Synergy HTX Hybrid Multi Mode Microplate Reader (BioTek Instruments, Inc., USA). Standard solutions of $NaNO_2$ in MC solutions and release medium were employed to obtain the calibration curves to correlate the absorbance values with the concentration.

2.3.2 Nitrate ions (NO_3^-). The concentration of NO_3^- was determined using a Nitrate Test Spectroquant® kit (1.09713.002, Sigma Aldrich, USA), based on the 2,6-dimethylphenol method, following the manufacturer's protocol. Absorbance measurement at λ = 320 nm was performed with a Synergy HTX Hybrid Multi Mode Microplate Reader. Standard solutions of KNO_3 in MC solutions and release media were prepared to obtain the calibration curves.

2.3.3 Hydrogen peroxide (H_2O_2). The determination of H_2O_2 concentration was performed using the Amplex™ Red reagent (Invitrogen™, Thermo Fisher Scientific, USA), in combination with horseradish peroxidase (HRP) (Sigma Aldrich, USA). Plasma treated MC solutions were diluted 1 : 100 in HP, and 50 μL of the Amplex red/HRP reagent were added to 200 μL of the diluted sample in a 96-well plate for incubation at 37 °C for 30 min. Fluorescence measurements were performed with a Synergy™ HTX Multi-Mode Microplate Reader using 560 nm and 590 nm as excitation and emission wavelengths, respectively. Standard solutions for the calibration curves to correlate fluorescence with concentration were prepared by diluting a 30 wt% H_2O_2 solution (Sigma Aldrich, USA).

2.3.4 Hydroxyl radicals (˙OH). The chemical probe coumarin (COU) (Sigma Aldrich, USA) was employed to detect ˙OH radicals. Different MC solutions were prepared in 1 mM COU, and different plasma-treatment times were evaluated. In solution, ˙OH radicals react with COU giving a fluorescent product: 7-hydroxycoumarin (hCOU). The fluorescence intensity of 500 μL of plasma treated MC solutions was measured with a Synergy™ HTX Multi-Mode Microplate Reader ($\lambda_{ex/em}$ = 360/460 nm). In order to calculate the production rate of this fluorescent product, standard solutions containing hCOU (Sigma Aldrich, USA) were prepared.

2.3.5 Stability of RONS in methylcellulose. To study the stability of the reactive species in MC, the concentrations of NO_2^-, NO_3^- and H_2O_2 after plasma treatment were measured again at 24 and 72 h after plasma treatment. In between measurements, the samples were stored in the fridge at 4 °C and only warmed up to room temperature for the quantification of RONS.

Moreover, the stability of these reactive species was also quantified for sample 1MC3.5HP after one gelling cycle: following plasma treatment, samples were gelled at 37 °C for 24 h in the incubator and subsequently cooled down at room temperature to solubilize again MC. Then, RONS were quantified following the procedure described in 2.3. This experiment was possible due to the thermoreversible properties of 1MC3.5HP.[26–28]

2.3.6 Release of RONS from the methylcellulose hydrogel. The ability of the MC hydrogel to release plasma-generated RONS was assessed in two different release media (PBS and complete Dulbecco's Modified Eagle's Medium (DMEM) (Gibco™, Carlsbad, CA, USA)). After gelation at 37 °C, plasma-treated samples were immersed in 1 mL of release medium and the concentration of NO_2^- and H_2O_2 released from the hydrogel was monitored by extracting a small amount of medium at different timepoints. A volume correction was taken into account and the quantification of the reactive species was conducted as explained in section 2.3. The concentration of NO_3^- was not quantified due to potential interactions of the release media with the chemical probe.[29]

2.4 Characterization of methylcellulose

2.4.1 Rheological properties. Rheological properties were assessed by means of dynamic oscillatory tests, using a rheometer (Discovery HR-2, TA Instruments) equipped with a 20 mm parallel plate geometry. The temperature was controlled using a Peltier plate. To prevent dehydration, the periphery of the samples was always covered by a thin layer of low viscosity oil. Steady-state flow experiments were performed in the range of 0.1 to 1000 s^{-1}. For the dynamic oscillatory tests, strain sweeps (0.1–1000%) before and after gelation were measured at 0.05 Hz frequency in order to determine the linear viscosity range (LVR). For the determination of the gel point, temperature ramp measurements (10–80 °C) were conducted at a heating rate of 1 °C min^{-1}, with an oscillation torque of 1 μN m to ensure shear strain values within the LVR. The storage modulus of 1MC3.5HP before and after plasma treatment was evaluated at 0.05 Hz frequency and 1 μN m oscillation torque. The heating rate was set to 2 °C min^{-1} and the measurements were conducted at 50 °C.

2.4.2 Microthermal analysis. A micro differential scanning calorimeter (micro DSC III, Setaram) was used to determine the thermal properties of MC solutions upon heating. Approximately, 700 mg of the sample were introduced to the sample cell and the reference cell was filled with the respective salt solution without MC. For one set of samples, the measurements were performed starting from the lowest salt concentration sample to minimize cross-contamination. The samples were heated from 10 °C to 80 °C at a heating rate of 1 °C min^{-1}.

2.4.3 Nuclear magnetic resonance (NMR). Proton nuclear magnetic resonance (^{1}H NMR) spectra acquired with a Bruker Advance 400 MHz spectrometer were employed to characterize MC. The MC solutions (both untreated and treated with plasma) were first lyophilized and then dissolved in deuterated dimethyl sulfoxide (dDMSO) (Sigma Aldrich, USA) at a concentration of 30 g L^{-1}. Spectra were recorded at 80 °C. Tetramethylsilane (δH: 0 ppm) and dDMSO (δH: 2.5 ppm) were used as reference for the spectra.

2.4.4 pH monitoring. The pH of both untreated and plasma-treated MC solutions was measured using an MM41 MultiMeter (Crison, Spain) with a Hanna HI1330B electrode (Hanna® instruments, USA).

2.4.5 Attenuated total reflectance – Fourier transformed infrared spectroscopy (ATR-FTIR). ATR-FTIR spectra of MC were recorded using a Nicolet 6700 spectrometer (Thermo Scientific), equipped with a Universal ATR sampling device with a germanium crystal. 15 μL of sample solution were placed directly onto the germanium crystal and we waited for the evaporation of the solvent. This process was repeated several times until a thin layer of MC was obtained. Spectra were acquired at room temperature in transmission mode as a function of the wavenumber ranging between 4000 and 675 cm^{-1}, with 64 scans at a resolution of 1 cm^{-1}. A background spectrum of air was collected under the same instrumental conditions before each series of measurements and subtracted from the sample spectra. To emphasize the potential effects of plasma-treatment on MC chemical structure, 1MC samples were diluted 1 : 10 (thus obtaining 0.1MC) before plasma-treatment and then analyzed as explained.

2.4.6 Thermal imaging. Noninvasive temperature measurements were effectuated by means of a thermal camera (GTC 400 C Professional, BOSCH, Germany), with an accuracy of ±3 °C, and a sensitivity of 0.1 °C. Images were taken at ~15 cm of the sample and the emissivity was set to 0.95.

2.4.7 Size exclusion chromatography (SEC). SEC measurements were carried out using a Shimadzu Prominence XR instrument equipped with an autosampler, a refractive index detector and a Shimadzu Shim-Pack Bio Diol-200 column (3 μm, 4.6 × 300 mm). The molecular weight range of the column is 4–300 kDa. The mobile phase was phosphate buffer (100 mM, pH 7.0) at a flow-rate of 0.5 mL min^{-1} and injection volume of 20 μL. 1MC samples were diluted 1 : 10 with phosphate buffer (thus obtaining 0.1MC) before plasma treatment and analyzed subsequently.

2.4.8 Swelling studies. After the gelation at 37 °C of 1MC3.5HP, the hydrogels were immersed in 1 mL of phosphate buffered saline (PBS, Biowest SAS) and a gravimetric assay was conducted to assess swelling behavior (n = 5). Swelling was determined using the following equation:

$$\%\ \text{swelling} = \frac{\text{hydrogel weight}(t) - \text{hydrogel weight}_{t=0}}{\text{hydrogel weight}_{t=0}} \times 100$$

where the hydrogel weight was calculated as the weight of the gelled hydrogel after 10 min, 30 min, 1 h, 2 h, 4 h, 6 h, 24 h and 72 h immersion. Samples were kept at 37 °C during the experiment.

2.5 Cell culture

The osteosarcoma cell line MG-63 (CRL-1427™, ATCC collection) was employed. Cells were maintained in Dulbecco's Modified Eagle's Medium (DMEM) (Gibco™, Carlsbad, CA, USA), supplemented with 10% fetal bovine serum (FBS) (Gibco™), 2 mM L-glutamine (Gibco™), 100 units per mL penicillin (Gibco™) and 100 μg mL^{-1} streptomycin (Gibco™), designated as "complete cell culture medium". Cells were maintained and expanded at 37 °C, 95% humidity and 5% CO_2. MC powder was sterilized by low-pressure plasma treatment using a low-pressure radio-frequency plasma (Femto plasma surface technologies, Diener Electronics, Germany) and the HP solutions were filtered at 37 °C using a 0.22 μm syringe filter (Millipore, Merck, Germany). All the processes leading to the preparation of 1MC3.5HP were carried out under sterile conditions.

2.5.1 Cell viability. Subconfluent MG-63 was trypsinized, centrifuged and seeded in a 24-well plate at a density of 2×10^4 cells per well, and incubated in 1 mL of complete culture medium. After 24 h adhesion, 150 μL of plasma-treated 1MC3.5HP (previously gelled 24 h at 37 °C) was added. Treatment times of 60, 180 and 300 s were investigated. Samples were incubated for 3 days, renewing the cell culture medium after the first day of incubation. Cell viability was evaluated at 24 and 72 hours with Presto Blue™ (Invitrogen, Carlsbad, CA, USA) and a LIVE/DEAD™ viability/cytotoxicity kit (Invitrogen, Carlsbad, CA, USA) following the supplier's protocol. Caspase-3 activity was evaluated at 24 h using the NucView® 488 Caspase-3 Substrate (Biotium, USA) as the manufacturer's protocol describes.

2.6 Statistical analysis

Comparison between multiple groups was made using one-way ANOVA. A two-tailed *t*-test was performed when two values were compared. *p*-values <0.05 were considered statistically significant.

3 Results and discussion

3.1 Gel point determination

The gel point of 1MC solutions with increasing concentrations of HP was evaluated by rheology tests and microDSC (Fig. 1i

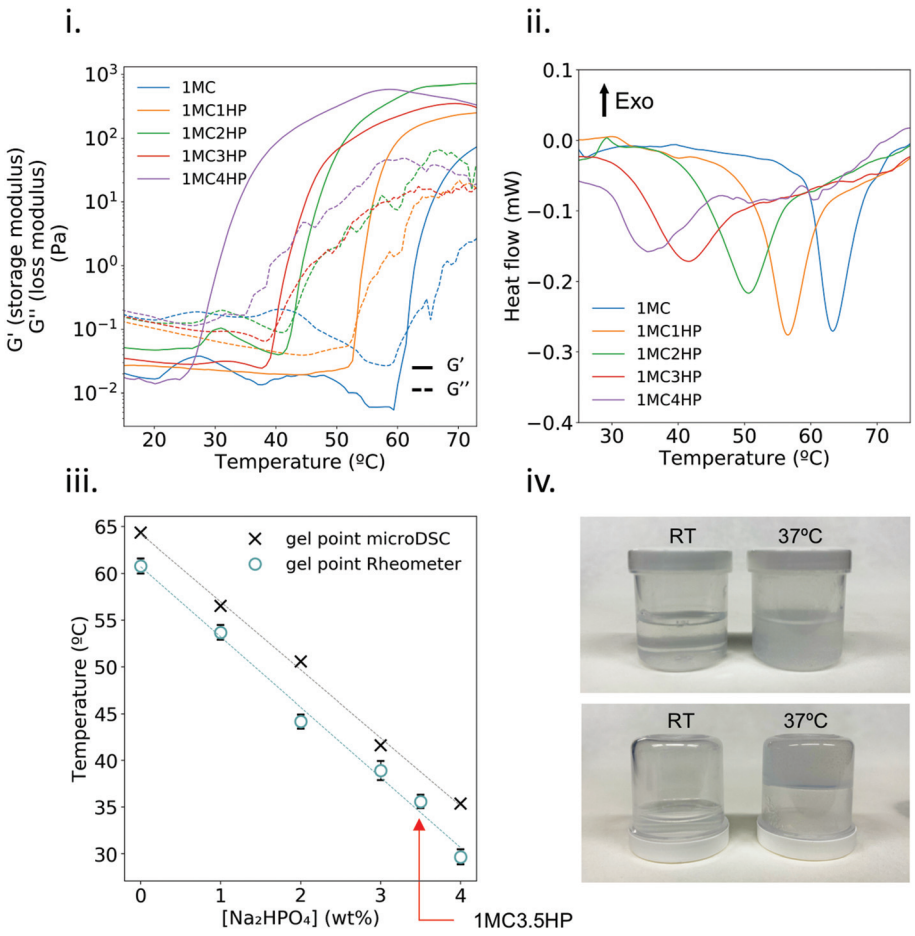

Fig. 1 Determination of the gel point for the different HP concentrations in 1MC. (i) Storage (*G'*) and loss (*G''*) modulus as a function of temperature and (ii) microDSC heating curves. In both cases the heating rate was 1 °C min^{-1}. (iii) Comparison of the gel point obtained by microDSC (n = 1) and rheological analysis (n = 2, except 1MC3.5HP; n = 4). Red arrow indicates the gel point of the 1MC3.5HP sample. (iv) Pictures of 1MC3.5HP at room temperature (RT) and after crosslinking at 37 °C.

and ii). In the rheology test, the crossover of storage modulus (G'') and loss modulus (G') was used as the indicator of the gel point,[19,30] whereas for the microDSC test, the gel point was determined at the endothermic peak of the microDSC curves. As expected, the higher the concentration of HP in the 1MC solution, the lower the gel point. The results obtained for both experiments are comparable (Fig. 1iii). The sample 1MC3.5HP was selected as the optimal composition since its gel point is at $T \approx 35.2$ °C – right below the physiological temperature (Fig. 1iv) – and was employed in subsequent experiments.

3.2 Characterization of methylcellulose after plasma treatment

A thermal camera was used to monitor the temperature of MC solutions during plasma treatment. Fig. 2i and ii show that, even though plasma treatment did increase the temperature of the well containing the sample, the temperature of MC solutions always remained below the crosslinking temperature, and thus staying in the liquid state, which was associated with a homogeneous treatment to the whole sample (Fig. S1†).

Temperature ramp measurements were conducted in order to determine the gel point of the plasma-treated hydrogel (Fig. 2iii) with no difference among treated and non-treated 1MC3.5HP. This indicates that plasma-treatment did not affect the crosslinking ability of the hydrogel.

The viscosity of 1MC3.5HP showed a shear-thinning behavior, in accordance with other studies (Fig. 2iv).[31,32] Although high variability was recorded at low shear stress, the viscosity of 1MC3.5HP did not significantly change due to the plasma-treatment. Similarly, storage modulus values did not vary either, meaning that the viscoelastic properties of the material remained unchanged after plasma-treatment (Fig. 2v). This indicates that the rheological properties of 1MC3.5HP – both before and after crosslinking – were not affected by plasma.

To further study changes in MC physico-chemical properties, SEC (Fig. 3i) was used to analyze pristine and plasma-treated 1MC diluted 1 : 10 before the treatment (0.1MC). Two peaks were detected in the chromatograms: peak A (at ~5.3 min) and peak B (at ~10.25 min). The former is attributed to the elution of the MC and the latter to the elution of the solvent. At increasing plasma-treatment time, peak A gradually shifted to higher elution times, reflecting a lower molecular weight. This effect was only observed for diluted samples (0.1MC) (Fig. S2†). This indicates that plasma treatment could only break up a small proportion of MC polymeric chains and was only appreciable in 0.1MC samples. Consequently, this minor reduction of molecular weight in MC did not have an influence in the rheological behavior of the material (Fig. 2iv and v). Since peak B is attributed to the lower limit of the column, the elution time at this point did not shift. However, the intensity of the peak increased at a higher plasma treatment time. This effect was attributed to changes in the refractive index of the solvent. A higher plasma-treatment time was related to a higher concentration of RONS in the solvent that led to higher intensity values.

ATR-IR and ^{1}H NMR spectroscopies were used to study any possible functional group modification or the generation of side products due to the interaction of plasma species with

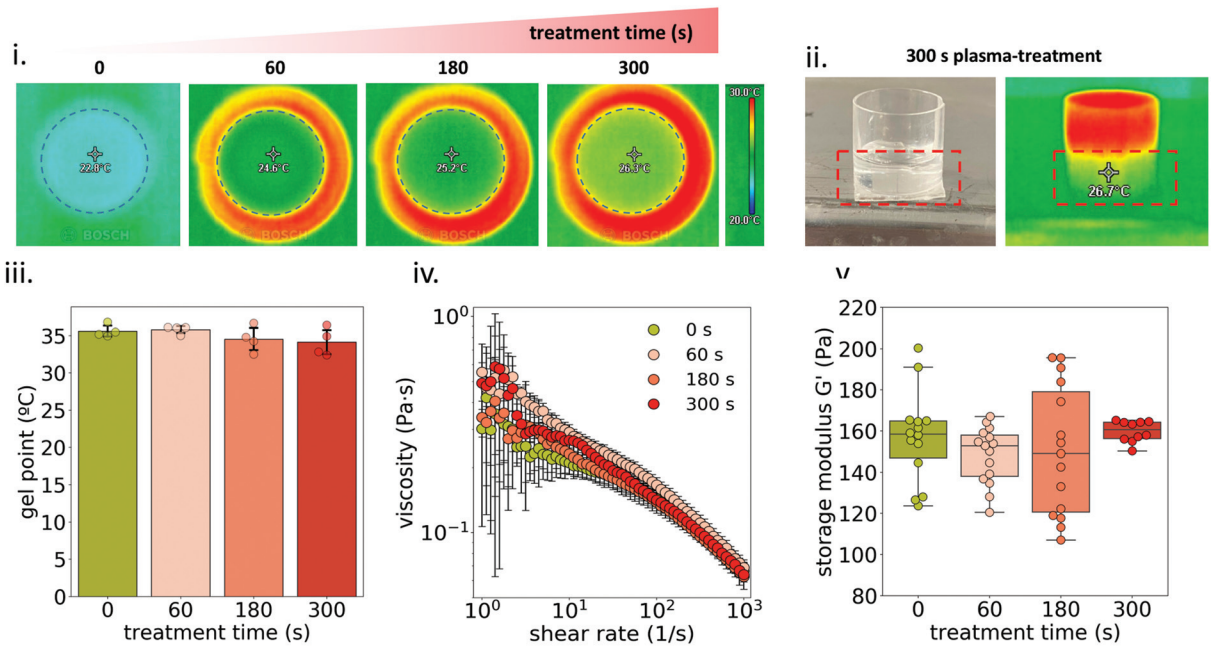

Fig. 2 Gel point and rheological analysis of plasma-treated 1MC3.5HP. (i) Thermal camera images of the surface of MC solutions after 60, 180 and 300 s plasma treatment. The temperature value is measured at the center of the well plate, right below the plasma jet plume. (ii) Thermal camera image of the side view of the well after 300 s plasma-treatment. (iii) Gel point comparison between non-treated and plasma-treated hydrogels. (iv) Viscosity curves of 1MC3.5HP at different plasma-treatment times before hydrogel formation. (v) Storage modulus (G') of 1MC3.5HP at different plasma-treatment times after hydrogel formation.

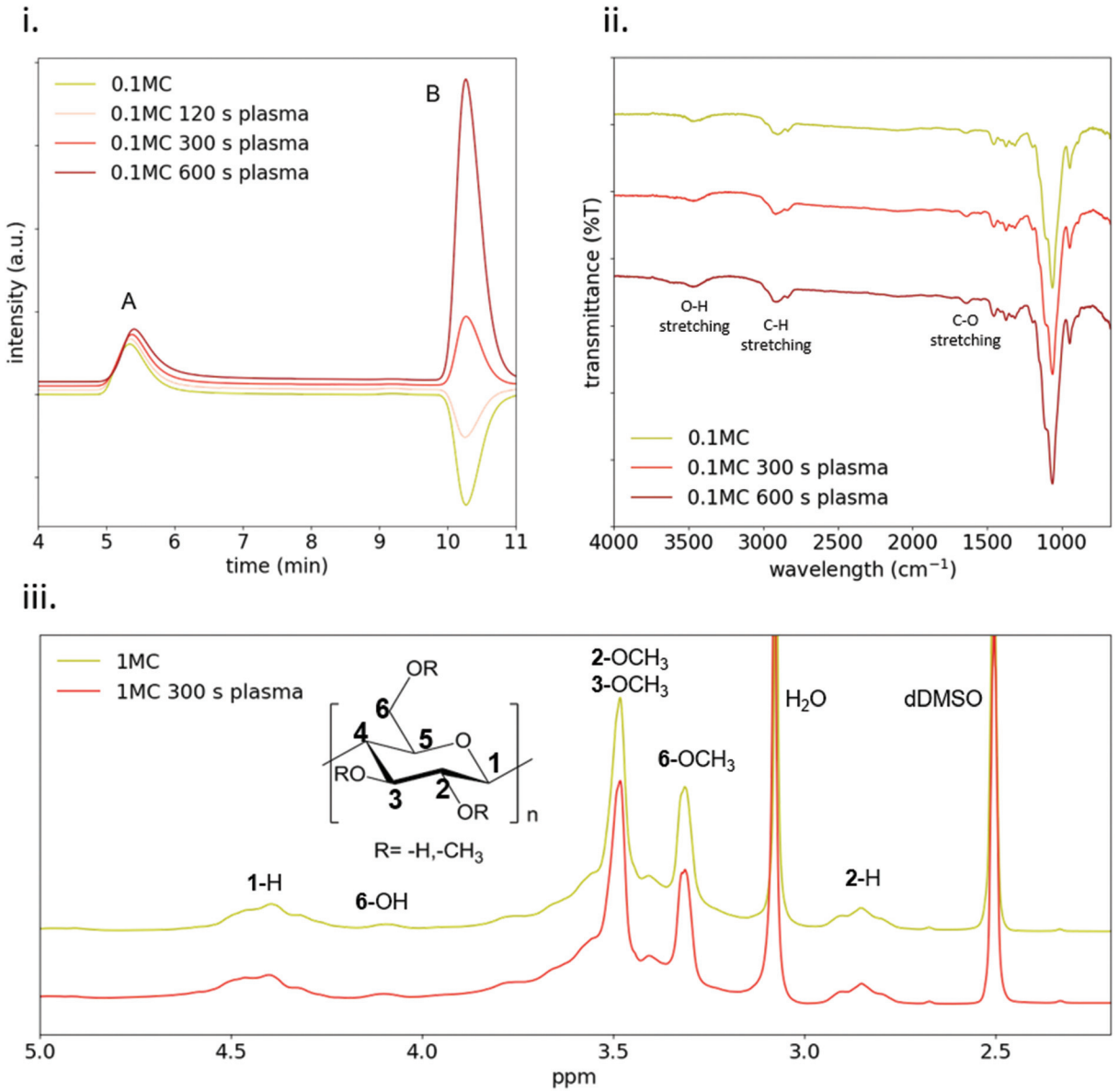

Fig. 3 Chemical characterization of plasma-treated MC. (i) Analysis by size exclusion chromatography of diluted (1 : 10) plasma-treated MC solutions. (ii) ATR-IR spectra of MC films at different plasma treatment times. (iii) ^{1}H NMR spectra of MC at different plasma treatment times (30 g L^{-1} in dDMSO at 80 °C).

MC. Fig. 3ii shows the ATR-IR spectra of both pristine and plasma-treated 0.1MC. The band at 3475 cm^{-1} is assigned to O–H stretching, and the bands at 2900 cm^{-1} and 1640 cm^{-1} to C–H stretching and C–O stretching, respectively.[33,34] The region from 1500 cm^{-1} to 500 cm^{-1} is considered the 'fingerprint' region of cellulose and cellulose derivatives.[35,36] No changes in absorbance were detected at any wavelength after plasma treatment. Moreover, no new absorbance bands were recorded, in agreement with previous studies that analyzed plasma-treated hydrogels by infrared spectroscopy.[13,16,37] Similar results were obtained with NMR spectroscopy (Fig. 3iii). The identification of the different peaks was performed as described in ref. 38–40. As shown, the spectrum of the pristine MC was the same as that for the plasma-treated sample. All these results strongly suggest that, at the concentrations used during the experiments, plasma treatment did not induce any evident functional group modification on the MC chemical structure.

3.3 Quantification and stability of RONS

The formation of NO_2^-, NO_3^- and H_2O_2 due to plasma treatment was quantified in three different liquids: 3.5HP, 1MC and 1MC3.5HP (Fig. 4i and ii). In all cases, these reactive species showed a linear increase in their concentration in the liquid with longer treatment times. The highest concentration values were obtained with 1MC3.5HP, generating ~75, ~165

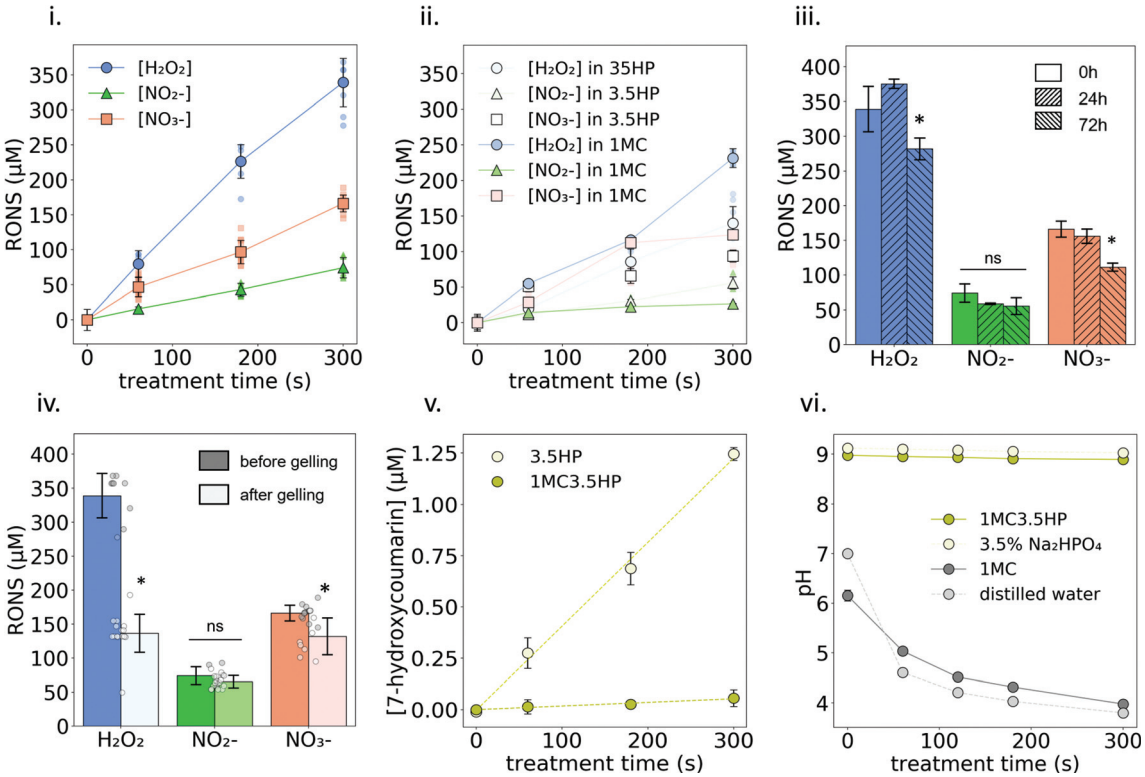

Fig. 4 Quantification and stability of plasma-generated RONS in 1MC35HP. (i) Concentration of H_2O_2, NO_2^- and NO_3^- in plasma treated 1MC3.5HP solution. Small markers represent each individual measure while big markers represent the mean value at each time point. (ii) Concentration of H_2O_2, NO_2^- and NO_3^- in plasma treated 1MC and 3.5HP solutions. (iii) Stability of RONS after 24 h and 72 h storage in the fridge. Asterisks denote statistically significant differences with respect to time 0 h (*$p < 0.05$). (iv) Stability of RONS after one gelling cycle. Asterisks denote statistically significant differences with respect to before gelling (*$p < 0.05$). (v) Indirect quantification of the production rate of OH radicals. (vi) pH evolution at increasing plasma treatment time of 1MC dissolved either in 3.5HP or in distilled water.

and ~340 μM NO_2^-, NO_3^- and H_2O_2, respectively, after 300 s of plasma treatment (Fig. 4i). These concentrations are in the same order of magnitude compared to other plasma-treated polysaccharide solutions (*i.e.* alginate[13]), while being several-fold larger than some typical isotonic saline solutions.[6,41,42] The shelf stability of these reactive species in 1MC3.5HP was monitored at 4 °C for up to 72 h. Only the concentration of H_2O_2 and NO_3^- experienced a slight reduction after 72 h storage at 4 °C (Fig. 4iii). In view of future clinical applications, it is of interest that plasma-treated hydrogels/liquids are stable during storage for a relatively long time. The concentration of H_2O_2 and NO_3^- in a plasma-treated water has been shown to be stable even after 21 days after treatment.[43] In contrast, it is known that the presence of some amino acids (such as cysteine and methionine) in plasma-treated liquids can drastically reduce the concentration of long-lived RONS during storage.[44] In our case, the polysaccharide chains of MC in solution did not have a significant impact on the stability of the reactive species, thus being a good substrate for the generation and stability of RONS for at least 48 h (Fig. 4i and iii).

However, when plasma-generated RONS were measured after one gelling cycle, the stability of H_2O_2 was clearly affected, to approximately half of its final concentration (Fig. 4iv). Incubation of the samples at the gelling temperature (37 °C) did not affect the stability of H_2O_2 without the presence of MC (Fig. S3†). Therefore, the formation of a hydrogel might be one of the reasons that led to H_2O_2 decomposition. The concentration of NO_3^- was slightly reduced to ~135 μM while NO_2^- did not experience any significant change in concentration.

Regarding short-lived reactive species, OH radicals were indirectly measured using a COU probe. As shown in Fig. 4v, the concentration of hCOU rises linearly with the increase of the plasma-treatment time. However, a much lower concentration is reached when the treated solution contains MC (see Fig. S4† for results with different MC concentrations). These results suggest that the presence of MC reduced the availability of OH radicals to react with the chemical probe. Nonetheless, the scavenging effect produced by MC on $^{\bullet}OH$ did not have an impact on the formation of NO_2^-, NO_3^- or H_2O_2. In fact, having MC in the solution slightly promoted the formation of H_2O_2 (Fig. 4i and ii). This suggests that H_2O_2 was not mainly formed by the combination of the dissolved OH radicals[45] but may rather come from secondary reactions involving OH radicals and the anhydroglucose units of MC. The differences observed due to the presence of MC in the concentration of NO_2^- and NO_3^- were not relevant (Fig. 4i and ii). Other biopolymer solutions[13–15] have also shown an increase in the for-

mation of NO_2^- and/or H_2O_2 upon plasma-treatment compared with solvent only, indicating an important secondary contribution to their generation that depends on the specific chemistry of the plasma-treated liquid/hydrogel.

The pH of 1MC rapidly decreased upon plasma treatment, leading to an acidic pH (pH ≈ 4) for the longest treatment time (Fig. 4vi). It is well known that plasma-treatment decreases the pH of non-buffered liquids mostly due to the generation of nitrous and nitric acid.[25] However, the pH values of 3.5HP and 1MC3.5HP remained constant (pH ≈ 9) due to the buffering effect of HP salt.

3.4 Swelling and release of RONS

The swelling behavior was assessed by immersing 1MC3.5HP in PBS at 37 °C, showing that the hydrogel could quickly take up around ~70% of its initial weight (Fig. 5i).

Two different media (PBS and complete culture medium (DMEM)) were used to quantify the release of RONS from the plasma-treated 1MC3.5HP. As observed in Fig. 5ii and iii, an initial burst release took place during the first hour of immersion in PBS, releasing ~80% of the initial amount of NO_2^- and H_2O_2. Then, the amount of these RONS remained constant following 24 h of experiment. This agrees with the release observed from the hydrogel containing NO_2^- and H_2O_2 added from standard solutions (Fig. S5†) that are released by diffusion. If compared to the concentrations of RONS quantified in DMEM, an ageing effect was observed when the release took place in this cell culture medium, as the amount of H_2O_2 decreased considerably after 24 h. As reported in ref. 44, some amino acids in cell culture medium have a clear effect on the stability of RONS. This was also observed in ref. 41, where the addition of FBS to a plasma treated liquid was related to a 30% decrease in the concentration of peroxides. This could be one of the reasons explaining why the concentration of NO_2^- and H_2O_2 decreased after 24 h in DMEM as it contains a high concentration of proteins.

It is important to highlight that both the swelling and release of RONS showed a very similar behaviour. Since water uptake kinetics are monitored by swelling, Fig. 5i indicates that water could diffuse into the 3D polymeric network of the MC hydrogel within the first hours of immersion until an equilibrium state was reached. Similarly, RONS could diffuse out to the release media from the 3D polymeric network and an equilibrium state was reached also within the first hours after immersion (Fig. 5ii and iii). Considering the small size of NO_2^- and H_2O_2, much below the hydrogel mesh size, the diffusion of these species out of the MC polymeric network was easy and, after 1 h immersion, RONS were completely released. Strategies might have to be considered in future to further slow down this release.

3.5 *In vitro* anticancer performance

Osteosarcoma cells MG-63 were exposed to plasma-treated 1MC3.5HP and cell viability was evaluated (Fig. 6). As shown in Fig. 6i, the non-treated MC hydrogel can be considered a biocompatible material, since no signs of cell death were observed. In contrast, the plasma-treated hydrogel reduced the metabolic activity of cancer cells in a treatment time-dependent manner, by inducing higher cytotoxicity at a longer plasma-treatment time (Fig. 6i and ii). Short treatment time (60 s) already showed a small reduction in the metabolic activity (~89%) after 24 h of exposure. These cells were able to recover after 72 h, increasing their metabolic activity up to levels similar to the control. However, at a long treatment time (300 s), a sharp decrease of the metabolic activity after 24 h (~35%) is observed, which further decreased (~20%) after 72 h.

Confocal images of Live/Dead assay were in agreement with cytotoxicity results, where the dose-response effect of plasma-treatment can be clearly observed (Fig. 6ii). This dose-response effect has already been reported by several authors employing different types of plasma-treated liquids as well as plasma-treated hydrogels.[45–47] In all cases, the cytotoxic effect of these treatments is based on the delivery of adequate concentrations of plasma-generated RONS to the cancer cell culture.[48,49] The oxidative stress generated by the supply of these exogenous RONS has been demonstrated to trigger specific biological pathways in cells that eventually lead to apoptosis.[50] In our

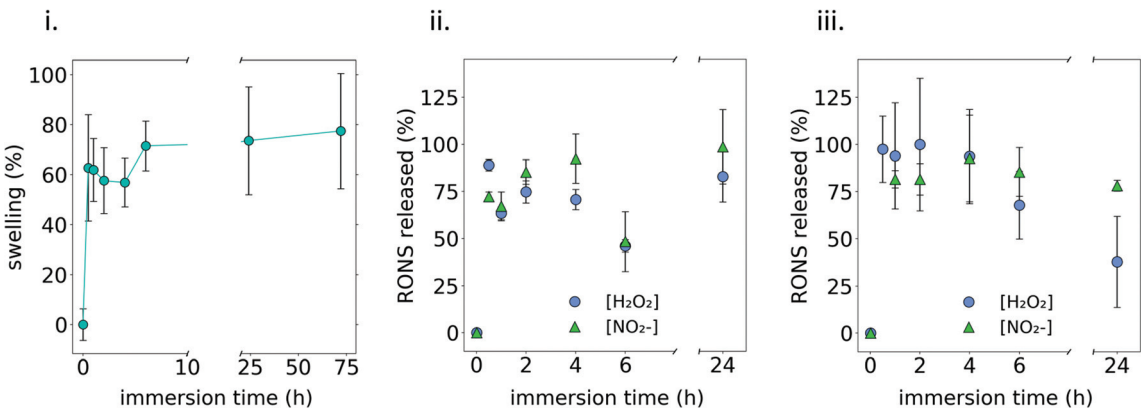

Fig. 5 Swelling of the hydrogel and release of plasma generated RONS in 1MC35HP. (i) Swelling of the 1MC3.5HP hydrogel after immersion in PBS at 37 °C. (ii) Release kinetics of plasma generated RONS after immersion of the 1MC3.5HP hydrogel in PBS at 37 °C. (iii) Release kinetics of plasma generated RONS after immersion of the 1MC3.5HP hydrogel in DMEM at 37 °C.

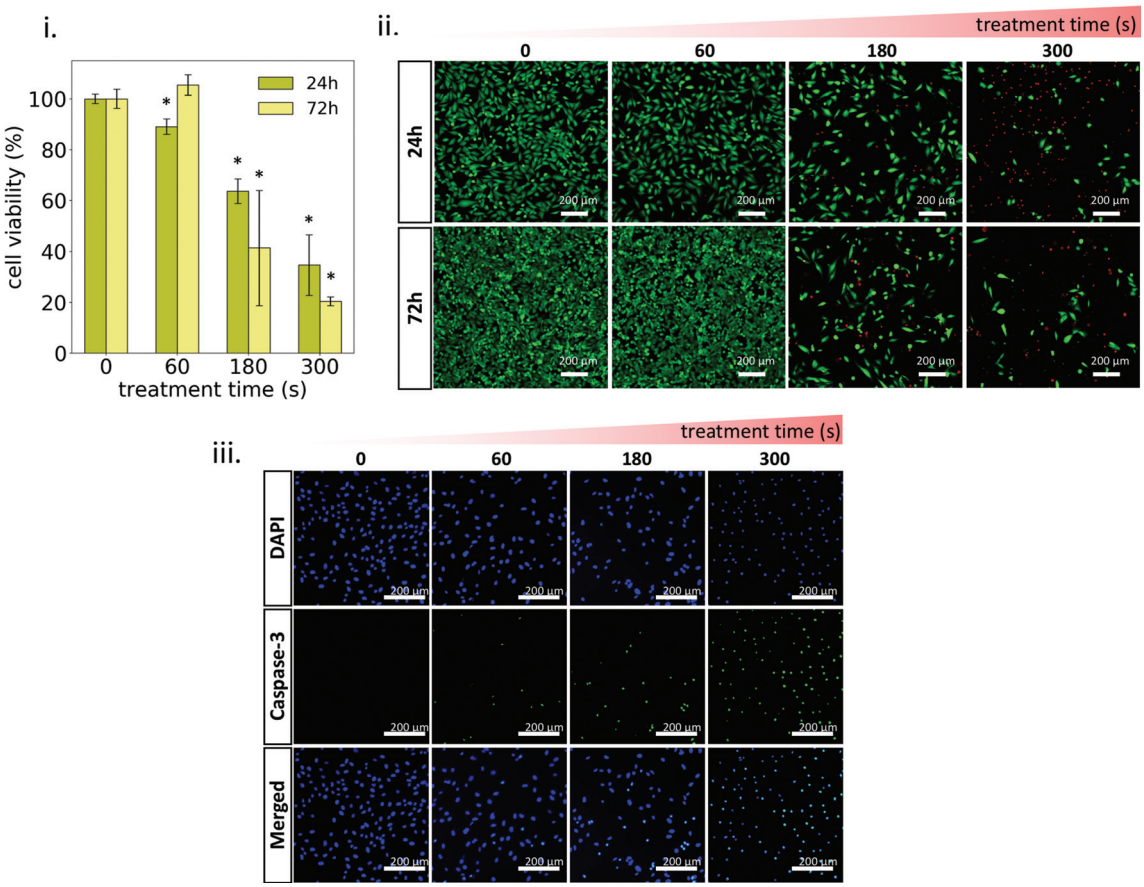

Fig. 6 Effects of the plasma-treated hydrogel on MG-63 cells. (i) Cell viability determined at 24 h and 72 h. (ii) Live/Dead assay showing live cells (green) and dead cells (red) after 24 h and 72 h exposure to the plasma-treated hydrogel. (iii) Caspase-3 activity after 24 h exposure to the plasma-treated hydrogel. Asterisks denote statistically significant differences with respect to the control (treatment time = 0 s) (*$p < 0.05$).

case, oxidative stress was induced by the release of RONS from the plasma-treated 1MC3.5HP (Fig. 5iii) and higher cytotoxic levels were obtained at a higher concentration of RONS in the culture medium (Fig. 5i and iii). Moreover, the reduced viability observed upon plasma treatment resulted in the activation of the apoptotic marker caspase-3 (Fig. 6iii). This marker showed higher activity at a higher plasma-treatment time, thus confirming the dose-response effect of plasma-treatment. Another sign of apoptotic cell death is chromatin condensation.[51,52] This was qualitatively detected for plasma-treated samples, since higher fluorescence intensities and smaller diameters of cell nuclei were observed (Fig. 6iii).

In all, the thermosensitive 1MC3.5HP hydrogel described here has clear advantages regarding the generation and the delivery of RONS to the cell culture. The concentration of RONS delivered by the hydrogel induced similar anticancer effects compared to several types of PTLs.

4 Conclusions

This work presents for the first time a thermosensitive MC hydrogel used as a delivery system of RONS generated by gas-plasma. The polymeric solution designed here (1MC3.5HP) is able to form a hydrogel at physiological temperatures while remaining a liquid at room temperature to allow plasma treatment and the formation of RONS. Although a minor fragmentation of the polymeric chains of MC was observed after plasma treatment, the rheological properties of the biomaterial were not affected, as happened also with its gelling ability. The anticancer effects of plasma-treated MC are time-dependent, showing increased cytotoxicity at longer plasma treatment times related to the higher concentration of RONS generated and released from the MC hydrogel.

Author contributions

Conceptualization: Xavi Solé-Martí, Cristina Canal. Data curation: Xavi Solé-Martí, Tània Vilella. Formal analysis: Xavi Solé-Martí, Tània Vilella, Cédric Labay, Francesco Tampieri. Investigation: Xavi Solé-Martí, Tània Vilella, Cédric Labay, Francesco Tampieri. Writing – original draft: Xavi Solé-Martí. Writing – review and editing: Cédric Labay, Francesco Tampieri, Maria-Pau Ginebra, Cristina Canal. Supervision:

Cristina Canal. Funding acquisition: Maria-Pau Ginebra, Cristina Canal.

Conflicts of interest

The authors declare no competing interests. Images created with BioRender.com

Acknowledgements

This project has received funding from the European Research Council (ERC) under the European Union's Horizon 2020 research and innovation program (grant agreement no. 714793). The authors acknowledge the financial support of MINECO for the PID2019-103892RB-I00/AEI/10.13039/501100011033 project. The authors belong to the SGR2017-1165. The authors acknowledge Generalitat de Catalunya for the Scholarship of Xavi Solé-Martí (2020 FI-B00999). Support for the research of Maria-Pau Ginebra and Cristina Canal was received through the ICREA Academia Award for excellence in research, funded by the Generalitat de Catalunya.

References

1 P. J. Bruggeman, M. J. Kushner, B. R. Locke, J. G. E. Gardeniers, W. G. Graham, D. B. Graves, R. C. H. M. Hofman-Caris, D. Maric, J. P. Reid, E. Ceriani, D. Fernandez Rivas, J. E. Foster, S. C. Garrick, Y. Gorbanev, S. Hamaguchi, F. Iza, H. Jablonowski, E. Klimova, J. Kolb, F. Krcma, P. Lukes, Z. Machala, I. Marinov, D. Mariotti, S. Mededovic Thagard, D. Minakata, E. C. Neyts, J. Pawlat, Z. L. Petrovic, R. Pflieger, S. Reuter, D. C. Schram, S. Schröter, M. Shiraiwa, B. Tarabová, P. A. Tsai, J. R. R. Verlet, T. Von Woedtke, K. R. Wilson, K. Yasui and G. Zvereva, *Plasma Sources Sci. Technol.*, 2016, **25**, 53002.

2 P. Bruggeman and C. Leys, *J. Phys. D: Appl. Phys.*, 2009, **42**, 53001.

3 Y. Li, T. Tang, H. J. Lee and K. Song, *Int. J. Mol. Sci.*, 2021, **22**, 3956.

4 E. Biscop, A. Lin, W. Van Boxem, J. Van Loenhout, J. De Backer, C. Deben, S. Dewilde, E. Smits and A. Bogaerts, *Cancers*, 2019, **11**, 1287.

5 R. Silva-Teixeira, M. Laranjo, B. Lopes, C. Almeida-Ferreira, A. C. Gonçalves, T. Rodrigues, P. Matafome, A. B. Sarmento-Ribeiro, F. Caramelo and M. F. Botelho, *Free Radicals Biol. Med.*, 2021, **171**, 302–313.

6 M. Mateu-Sanz, J. Tornín, B. Brulin, A. Khlyustova, M. P. Ginebra, P. Layrolle and C. Canal, *Cancers*, 2020, **12**, 227.

7 X. Solé-Martí, A. Espona-Noguera, M. P. Ginebra and C. Canal, *Cancers*, 2021, **13**, 1–17.

8 Z. Chen, H. Simonyan, X. Cheng, E. Gjika, L. Lin, J. Canady, J. H. Sherman, C. Young and M. Keidar, *Cancers*, 2017, **9**, 1–16.

9 F. Saadati, H. Mahdikia, H. A. Abbaszadeh, M. A. Abdollahifar, M. S. Khoramgah and B. Shokri, *Sci. Rep.*, 2018, **8**, 7689.

10 F. Utsumi, H. Kajiyama, K. Nakamura, H. Tanaka, M. Mizuno, K. Ishikawa, H. Kondo, H. Kano, M. Hori and F. Kikkawa, *PLoS One*, 2013, **8**, 81576.

11 K. R. Liedtke, S. Bekeschus, A. Kaeding, C. Hackbarth, J. P. Kuehn, C. D. Heidecke, W. Von Bernstorff, T. Von Woedtke and L. I. Partecke, *Sci. Rep.*, 2017, **7**, 8319.

12 K. R. Liedtke, E. Freund, C. Hackbarth, C. D. Heidecke, L. I. Partecke and S. Bekeschus, *Clin. Plasma Med.*, 2018, **11**, 10–17.

13 C. Labay, I. Hamouda, F. Tampieri, M. P. Ginebra and C. Canal, *Sci. Rep.*, 2019, **9**, 16160.

14 C. Labay, M. Roldán, F. Tampieri, A. Stancampiano, P. E. Bocanegra, M. P. Ginebra and C. Canal, *ACS Appl. Mater. Interfaces*, 2020, **12**, 47256–47269.

15 X. Solé-Martí, C. Labay, Y. Raymond, J. Franch, R. Benitez, M.-P. Ginebra and C. Canal, Submitted for Publication.

16 H. Zhang, S. Xu, J. Zhang, Z. Wang, D. Liu, L. Guo, C. Cheng, Y. Cheng, D. Xu, M. G. Kong, M. Rong and P. K. Chu, *Biomaterials*, 2021, **276**, 121057.

17 M. H. Kim, B. S. Kim, H. Park, J. Lee and W. H. Park, *Int. J. Biol. Macromol.*, 2018, **109**, 57–64.

18 M. C. Tate, D. A. Shear, S. W. Hoffman, D. G. Stein and M. C. LaPlaca, *Biomaterials*, 2001, **22**, 1113–1123.

19 M. K. Bain, B. Bhowmick, D. Maity, D. Mondal, M. M. R. Mollick, D. Rana and D. Chattopadhyay, *Int. J. Biol. Macromol.*, 2012, **51**, 831–836.

20 N. Li, E. Liu and C. H. Lim, *J. Phys. Chem. B*, 2007, **111**, 6410–6416.

21 S. Q. Liu, S. C. Joshi and Y. C. Lam, *J. Appl. Polym. Sci.*, 2008, **109**, 363–372.

22 J. Tornin, C. Labay, F. Tampieri, M. P. Ginebra and C. Canal, *Nat. Protoc.*, 2021, **16**, 2826–2850.

23 I. Guevara, J. Iwanejko, A. Dembińska-Kieć, J. Pankiewicz, A. Wanat, P. Anna, I. Gołąbek, S. Bartuś, M. Malczewska-Malec and A. Szczudlik, *Clin. Chim. Acta*, 1998, **274**, 177–188.

24 M. J. Moorcroft, J. Davis and R. G. Compton, *Talanta*, 2001, **54**, 785–803.

25 A. Khlyustova, C. Labay, Z. Machala, M. P. Ginebra and C. Canal, *Front. Chem. Sci. Eng.*, 2019, **13**, 238–252.

26 M. Takahashi, M. Shimazaki and J. Yamamoto, *J. Polym. Sci., Part B: Polym. Phys.*, 2001, **39**, 91–100.

27 S. Morozova, M. L. Coughlin, J. T. Early, S. P. Ertem, T. M. Reineke, F. S. Bates and T. P. Lodge, *Macromolecules*, 2019, **52**, 7740–7748.

28 S. A. Arvidson, J. R. Lott, J. W. McAllister, J. Zhang, F. S. Bates, T. P. Lodge, R. L. Sammler, Y. Li and M. Brackhagen, *Macromolecules*, 2013, **46**, 300–309.

29 V. Veronico, P. Favia, F. Fracassi, R. Gristina and E. Sardella, *Plasma Processes Polym.*, 2021, **18**, 2100062.

30 L. Li and Y. Aoki, *Macromolecules*, 1997, **30**, 7835–7841.

31 L. Deng, Y. Liu, L. Yang, J. Z. Yi, F. Deng and L. M. Zhang, *Colloids Surf., B*, 2020, **194**, 111159.

32 K. K. Tha Goh, M. S. Mei Wee and Y. Hemar, *Food Funct.*, 2013, **4**, 627–634.
33 G. R. Filho, R. M. N. de Assunção, J. G. Vieira, C. da S. Meireles, D. A. Cerqueira, H. da Silva Barud, S. J. L. Ribeiro and Y. Messaddeq, *Polym. Degrad. Stab.*, 2007, **92**, 205–210.
34 M. Baiardo, G. Frisoni, M. Scandola and A. Licciardello, *J. Appl. Polym. Sci.*, 2002, **83**, 38–45.
35 R. G. Zhbankov, *Infrared Spectra of Cellulose and its Derivatives*, Springer US, Boston, MA, 1995.
36 H. Akinosho, S. Hawkins and L. Wicker, *Carbohydr. Polym.*, 2013, **98**, 276–281.
37 Z. Liu, Y. Zheng, J. Dang, J. Zhang, F. Dong, K. Wang and J. Zhang, *ACS Appl. Mater. Interfaces*, 2019, **11**, 22941–22949.
38 P. L. Nasatto, F. Pignon, J. L. M. Silveira, M. E. R. Duarte, M. D. Noseda and M. Rinaudo, *Polymers*, 2015, **7**, 777–803.
39 Y. Sekiguchi, C. Sawatari and T. Kondo, *Polym. Bull.*, 2002, **47**, 547–554.
40 M. Karakawa, Y. Mikawa, H. Kamitakahara and F. Nakatsubo, *J. Polym. Sci., Part A: Polym. Chem.*, 2002, **40**, 4167–4179.
41 J. Tornín, A. Villasante, X. Solé-Martí, M. P. Ginebra and C. Canal, *Free Radicals Biol. Med.*, 2021, **164**, 107–118.
42 K. R. Liedtke, E. Freund, M. Hermes, S. Oswald, C. D. Heidecke, L. I. Partecke and S. Bekeschus, *Cancers*, 2020, **12**, 123.
43 I. E. Vlad and S. D. Anghel, *J. Electrost.*, 2017, **87**, 284–292.
44 D. Yan, N. Nourmohammadi, K. Bian, F. Murad, J. H. Sherman and M. Keidar, *Sci. Rep.*, 2016, **6**, 26016.
45 N. K. Kaushik, B. Ghimire, Y. Li, M. Adhikari, M. Veerana, N. Kaushik, N. Jha, B. Adhikari, S. J. Lee, K. Masur, T. Von Woedtke, K. D. Weltmann and E. H. Choi, *Biol. Chem.*, 2018, **400**, 39–62.
46 Y. Sato, S. Yamada, S. Takeda, N. Hattori, K. Nakamura, H. Tanaka, M. Mizuno, M. Hori and Y. Kodera, *Ann. Surg. Oncol.*, 2018, **25**, 299–307.
47 D. Yan, J. H. Sherman and M. Keidar, *Anticancer Agents Med. Chem.*, 2017, **18**, 769–775.
48 D. Yan, A. Talbot, N. Nourmohammadi, X. Cheng, J. Canady, J. Sherman and M. Keidar, *Sci. Rep.*, 2015, **5**, 1–17.
49 G. Bauer, *Redox Biol.*, 2019, **26**, 101291.
50 M. Mateu-Sanz, J. Tornín, M. P. Ginebra and C. Canal, *J. Clin. Med.*, 2021, **10**, 1–29.
51 D. Gümbel, S. Bekeschus, N. Gelbrich, M. Napp, A. Ekkernkamp, A. Kramer and M. B. Stope, *Int. J. Mol. Sci.*, 2017, **18**, 2004.
52 G. Majno and I. Joris, *Am. J. Pathol.*, 1995, **146**, 3–15.